

# FUTURE GALAXY CLUSTER SURVEYS: THE EFFECT OF THEORY UNCERTAINTY ON CONSTRAINING COSMOLOGICAL PARAMETERS

E.S. LEVINE<sup>1</sup>, A.E. SCHULZ<sup>2</sup>, MARTIN WHITE<sup>1</sup>

<sup>1</sup>Department of Astronomy, University of California, Berkeley, CA 94720

<sup>2</sup>Department of Physics, Harvard University, Cambridge, MA 02138

*Draft version October 29, 2018*

## ABSTRACT

Using the Fisher matrix formalism, we quantitatively investigate the constraints on a 10 dimensional space of cosmological parameters which may be obtained with future cluster surveys. We explore the dependence of the  $\Omega_m$  constraint on both angular coverage and depth of field. We show that in each case there is a natural cutoff beyond which the constraints on  $\Omega_m$  do not significantly improve. We also investigate the sensitivity of the constraints to changes in our knowledge of the Mass-Temperature (M-T) relation by including its normalization and scatter as two of the parameters in the Fisher matrix. To make our analysis more realistic, we have added, as priors, the Fisher matrices from hypothetical supernova and CMB experiments. We find that X-ray cluster surveys actually help to constrain the M-T relation, and explore the implications of this result.

*Subject headings:* Galaxies-clusters, cosmology-theory

## 1. INTRODUCTION

One of the most puzzling mysteries in cosmology today is the nature of the dark energy, believed to be driving the accelerated expansion of the universe. This constituent is predicted to be smooth, except possibly on horizon scales, so its cosmological effects are observed solely through its influence on the expansion rate,  $H$ . Since the expansion is accelerating, the dark energy equation of state  $w_\phi = P_\phi/\rho_\phi < 0$ . Assuming that the equation of state varies slowly with time, the dark energy component must only recently have become cosmologically significant. In order to best constrain this component, it is therefore desirable to probe the redshift range  $0 < z \lesssim 2$ .

Several authors have suggested using counts of clusters of galaxies to probe the evolution of the dark energy in this redshift range (Haiman *et al.* 2000; Kneissl *et al.* 2002; Huterer & Turner 2001; Podariu & Ratra 2001; Newman *et al.* 2002). Because these number counts depend on the growth function as well as on the proper distance probed by Type Ia Supernovae (SNe) and Cosmic Microwave Background (CMB) experiments, a cluster survey will yield a constraint complementary to constraints from those experiments. Another advantage is that clusters are big, bright, and sparse enough to make surveys of large volumes relatively tractable.

Many factors affect our ability to extract constraints on cosmological parameters from a cluster survey. In this paper we examine the trade-offs in parameter estimation between conducting a narrow deep survey which may require intimate knowledge of the nature of the dark energy, and a broad shallow survey which may not. This is because shallow surveys use the evolution of the cluster mass function to constrain primarily  $\Omega_m$ , and are much less sensitive to  $\Omega_\phi$  or the equation of state,  $w_\phi$ . In this case, the interpretation of the cluster counts will be relatively free of the modeling parameters. On the flip side, once several of the other parameters are determined reasonably accurately by combining a shallow survey with CMB and SNe

constraints, a deep cluster survey will be crucial if one hopes to measure any evolution in the equation of state.

Considering the explosion of cluster survey activity that will occur in the next few years, it will be important to either resolve or work around the theory uncertainties in order to make the best use of the imminent data. One problem that must be examined is how to relate the observable quantity (e.g. cluster X-ray gas temperature) to the quantity predicted by the cosmological theory (usually mass). In this paper we determine quantitatively how uncertainties in the Mass-Temperature (M-T) relation and in the nature of the dark energy will affect the optimal constraints, and in light of that information, identify the most effective types of cluster surveys to carry out. Finally, accepting the current limitation of the theory, we show how the constraints depend on the total number of clusters and implicitly on the limiting mass of the survey.

## 2. BACKGROUND

There is a long history of using various cosmological tests to constrain parameters in different directions of parameter space. Often an observation will not be particularly useful in constraining an individual parameter, but will rather nicely constrain a sum or product of parameters. The downside is that usually there is another combination of parameters which is very poorly constrained; a degeneracy orthogonal in parameter space to the best constrained combination. To break the degeneracy, we can combine the constraint with other cosmological experiments. The key element in obtaining a narrow region of likelihood contour intersection is finding observables that each have a different dependence on the cosmological parameters.

Much progress has been made in constraining the rather large set of parameters typically present in today's cosmological models. One of the most important constraints comes from observations of the CMB. Existing CMB experiments (Smoot *et al.* 1992; Miller *et al.* 1999; de Bernardis *et*

*al.* 2001; Hanany *et al.* 2000; Padin *et al.* 2001; Pryke *et al.* 2001) have already yielded information about the initial conditions at the time of last scattering, and have made some progress in determining the physical matter and baryon densities:  $\Omega_m h^2$ ,  $\Omega_b h^2$ , and the angular distance to the last-scattering surface  $r_\theta$ . Now with the upcoming *MAP* and *Planck* missions, the CMB anisotropies will be studied with increasing precision, and the constraints will be improved by incorporating new data on the polarization of the CMB. The three primary parameters mentioned above will be measured to accuracies approaching 1%, with auxiliary parameters including the equation of state  $w_\phi$ , measured to accuracies a few times worse than this (Hu *et al.* 1999).

The constraint on  $r_\theta$  can be interpreted as essentially fixing one combination of the matter and dark energy densities and the evolution of the dark energy. However, even when we impose the condition  $\Omega_k = 0$ , there are still degeneracies that exist between  $\Omega_m$  and the Hubble parameter, and to a smaller extent, the equation of state of the dark energy,  $w_\phi$ .

There is a well known complementarity between the CMB constraints and constraints from type Ia supernovae observations which one can take advantage of to break these degeneracies (White 1998, Tegmark *et al.* 1998, Permuter *et al.* 1999, Hu *et al.* 1999). The supernova constraints also come from a distance measure, but in parameter space they are orthogonal to the constraints from the CMB because the distance involved is much smaller than the distance to the last scattering surface, from which all of the CMB photons originate. Thus for example, in measuring the energy densities of the matter and the dark energy, the constraint from the Type Ia Supernovae measures  $\Omega_m - \Omega_\phi$ , whereas the CMB measures a weighted sum of  $\Omega_m + \Omega_\phi$  (Cohn 1998). The effect is not quite as pronounced in the  $\Omega_m - w_\phi$  plane, but it seems clear that supernovae will provide a strong complementary measurement. The intersection of the likelihood contours from a supernova experiment such as SNAP with CMB constraints obtained using PLANCK could determine the matter density to 3.3% if the polarization information is included (e.g. Tegmark *et al.* 1998). An analysis of the optimal survey strategy for Supernovae searches has been carried out by Spergel & Starkman (2002), who determined that intermediate redshifts of 0.3 – 0.4 are the best ones to probe when combining the Supernova results with the CMB.

Although supernovae do seem to provide a clear way to narrow the parameter space, it would be a very valuable cross check if a third observable was found whose likelihood contours intersected the other two in the same region of parameter space. Such an independent constraint could additionally remove one of the largest degeneracies in determining the equation of state and its time evolution. A promising observable to study is the number density of rich galaxy clusters as a function of redshift, an idea which was suggested as early as 1992 by Oukbir & Blanchard (1992) among others. Studying the number density would provide an orthogonal constraint because in addition to being sensitive to the comoving distance measure, it is also sensitive to the rate of growth of fluctuations and

hence the matter density  $\Omega_m$  (in units of the critical density,  $\rho_{\text{crit}} = 3H_0^2/8\pi G$ , where  $H_0 = 100h \text{ km s}^{-1} \text{ Mpc}^{-1}$  is the Hubble constant). In models with a lower matter density, the growth of structure ceases earlier. When normalized to the same level of fluctuations today, this implies larger fluctuations at earlier times. If the number density of objects is related to the amplitude of fluctuations on a length scale  $R \propto M^{1/3}$ , as in the Press-Schechter theory or its generalizations (Press & Schechter 1974), then this predicts more clusters of a given mass at high- $z$  in models with a low  $\Omega_m$ . This method has been tested numerically by many authors (Efstathiou *et al.* 1988, Efstathiou & Rees 1988, White *et al.* 1993, Lacey & Cole 1994, Gelb & Bertschinger 1994, Bond & Myers 1996, Eke *et al.* 1996, Sheth & Tormen 1999, and Jenkins *et al.* (2001)), and it was found that the formalism accurately predicts the abundance of rich clusters as a function of redshift for a broad range of different cosmologies.

Unfortunately, there are still many factors that present difficulties when attempting to use a cluster survey to constrain the cosmological parameters. A recent study (Viana & Liddle 1999) concluded that when all of the major sources of error both in theory and observation are accounted for, an unambiguous determination of the matter density  $\Omega_m$  is not yet possible. One complication is that the model of the evolution of the dark energy equation of state is not well determined by any other observations. This makes it difficult to interpret the impact of observed evolution of the number density with redshift on the parameter  $\Omega_m$ , because it becomes entangled with  $w_\phi(z)$ .

Upcoming studies will introduce a golden age in cluster surveys. Several observational programs will replace the current catalog of tens of clusters at intermediate redshifts ( $z < 1$ ) with thousands of detections improving not only the quantity, but the quality of the available data. With the launch of the *XMM/Newton* and *Chandra* satellites, the study of X-ray emission from the IGM has dramatically advanced. The XMM (X-ray Multi Mirror Satellite) Large-Scale Structure Survey (Pierre, Valtchanov & Refregier 2002) will map the location of clusters and groups of galaxies out to  $z \approx 1$  over an  $8^\circ \times 8^\circ$  area. This survey alone is expected to detect up to 800 clusters in the temperature band ranging from 0.4 to 4 keV. Another proposed survey using the same instrument, the XMM Cluster Survey (XCS; Romer *et al.* 2001), is expected to cover  $\approx 800 \text{ deg}^2$  and include more than 8000 clusters, as many as 1800 of which will have well-defined temperatures (estimates for  $\Omega_m = 0.3, \Omega_\phi = 0.7$ ) with  $T > 2 \text{ keV}$ . There should even be a significant number detected with  $z > 1$ .

Meanwhile, surveys for clusters are now being carried out at optical wavelengths (using both galaxy counts and weak lensing) and using the Sunyaev-Zel'dovich effect (Sunyaev & Zel'dovich 1980). In the more distant future, the Planck satellite has the potential to find  $10^4$  clusters (with some dependence on cosmology) out to  $z \sim 1$ . This enormous quantity of upcoming cluster survey work motivates our study to find survey parameters that optimize the constraints on cosmological parameters.

### 3. METHOD

In order to address these questions we make use of the Fisher matrix formalism (see Tegmark *et al.* 1996 for a pedagogical review). This allows us to elucidate the dependence of our hypothetical constraints on both our survey design and our theoretical uncertainty, highlighting the role of parameter degeneracies. Because we have chosen to use the Fisher matrix, expressed in terms of the derivatives of the likelihood function at the maximum, rather than a full likelihood analysis, all of our constraints are “local” rather than global. This should not affect any of our conclusions.

To make our analysis more relevant to the future where CMB and SNe surveys have progressed significantly, we consider the constraints from a combination of hypothetical observations. First we have a cluster survey, but we include as ‘prior’ information the Fisher matrices obtained from a mock MAP mission and a future SNe survey. We describe each of these pieces below.

#### 3.1. Assembling the cluster Fisher matrix.

We assume a flat cosmology and have chosen as our basis of parameters the space ( $\Omega_m = 0.3$ ,  $h = .67$ ,  $\Omega_b h^2 = 0.018$ ,  $n_s = 1$ ,  $w_\phi = -1$ ,  $\delta_H = 5.02 \times 10^{-5}$ ,  $T/S = 0$ ,  $\tau = .2$ , M-T normalization =  $6.59 \times 10^{-10}$ ,  $\sigma_{M-T} = .1$ ). The quantities M-T normalization and  $\sigma_{M-T}$  are defined below in §3.2.

If we bin narrowly in the observable temperature and in redshift, the abundance of clusters is naturally described by a Poisson distribution, and so the Fisher matrix  $\mathbf{F}$  becomes (Holder *et al.* 2001)

$$\mathbf{F}_{ij} = -\frac{\partial^2 \ln \mathcal{L}}{\partial \theta_i \partial \theta_j} = \sum_{a=1}^S \frac{\partial N_a}{\partial \theta_i} \frac{\partial N_a}{\partial \theta_j} \frac{1}{N_a} \quad (1)$$

where the sum runs over  $S$  bins, chosen to be sufficiently small that our fiducial model predicts  $N_a \ll 1$  clusters per bin. In practice, binning in redshift finer than  $\Delta z = 0.01$  does not change the constraints significantly. Here  $\mathcal{L}$  is the likelihood function, the  $\theta_i$  are the cosmological parameters and  $N_a$  is the number of clusters expected in bin  $a$ . The derivatives are evaluated at the position of the fiducial model in likelihood space logarithmically via the rule:

$$g'(\theta_i) = \frac{g(\theta_i \times \Delta\theta) - g(\theta_i \div \Delta\theta)}{2\theta_i \ln(\Delta\theta)}. \quad (2)$$

All derivatives were found to converge with  $\Delta\theta = 1.0001$ . When varying  $\Omega_m$  we also varied  $\Omega_\Lambda$  to maintain  $\Omega_k = 0$ . The dependence on the cosmological parameters enters through the mass function  $dn/dM$ . We use the fitting function of Jenkins *et al.* (2001),

$$\frac{dn}{dM} = -\frac{\rho_m}{M^2} \frac{d \ln \sigma}{d \ln M} \left[ 0.315 \exp \left[ -(-\ln \sigma + 0.61)^{3.8} \right] \right] \quad (3)$$

where  $\rho_m$  is the mean background matter density, and  $\sigma^2$  is the variance of the mass, filtered on some scale  $R(M)$ . It contains all the details of the cosmological model through its dependence on the power spectrum  $P(k)$ :

$$\sigma^2 = \int_0^\infty 4\pi k^2 dk \widehat{W}^2(k) P(k) \quad (4)$$

We have chosen a spherical top hat (in real space) as our smoothing window, with Fourier transform  $\widehat{W}$ . We use a power-law primordial power spectrum and the fits to the transfer function of Eisenstein & Hu (1997).

Using the M-T relation, along with its associated Gaussian scatter, we map the number densities by mass,  $n(M)$ , to number densities by temperature,  $n(T)$ . We construct the Fisher matrix only from bins with a temperature greater than a certain threshold; this corresponds to the detection threshold of actual surveys. Though the majority of our analysis is done with a threshold of 5 keV, we also explore the tradeoffs behind choosing different temperature thresholds. One benefit of this method is that since the volume at a given redshift scales linearly with angular survey size, so too does the number of clusters expected for a given temperature range. Therefore, we have the relation  $N_a = n_a V$ , where  $V$  represents some number of  $(h^{-1} \text{Mpc})^3$  and  $n_a$  is the number of clusters per  $(h^{-1} \text{Mpc})^3$ . This identity allows us to rewrite (1):

$$\mathbf{F}_{ij} = V \sum_{a=1}^S \frac{\partial n_a}{\partial \theta_i} \frac{\partial n_a}{\partial \theta_j} \frac{1}{n_a}. \quad (5)$$

As  $V$  is proportional to the angular survey area, multiplying the area by some factor corresponds to multiplying each Fisher matrix element by the same factor. We will take advantage of this below.

#### 3.2. Constructing the M-T relation

For the cluster  $M-T$  relation we take the ‘virial’ relation (Kaiser 1986; Peacock 1999)

$$T \propto M_{\text{vir}}^{2/3} H^{2/3}(z) \Delta^{1/3}(z) h^{2/3} \quad (6)$$

which can be derived by assuming clusters are self-similar, pressure supported, isothermal spheres. Here  $M_{\text{vir}}$  represents the virial mass of the cluster,  $\Delta(z)$  is the mean interior overdensity, relative to the critical density, for which we say the object has virialized.  $\Delta$  is the familiar factor  $18\pi^2$  for an  $\Omega_m = 1$  universe, and otherwise is given by the fitting function found by Bryan & Norman (1986).

We fix the normalization of the M-T relation by appealing to numerical simulations. However, the normalization constant could potentially vary across different cosmologies. A comprehensive summary of all the different calculations of the normalization is found in Henry (2000) and Pierpaoli, Scott, & White (2001). Since we will compensate for differences in  $h$ , the parameters we should be concerned with are  $\Omega_m$  and  $\Omega_b$ . We will use the value quoted by Eke *et al.* (1998) (hereafter ENF),

$$T = 6.59 \left( \frac{M}{10^{15} M_\odot} \right)^{2/3} \text{ keV} \quad (7)$$

with a Gaussian scatter of  $\sigma_{M-T} = 13.33\%$ , because the cosmology they simulate is very close to our fiducial model ( $\Omega_m = 0.3$ ,  $\Omega_\Lambda = 0.7$ ,  $h = 0.7$ ,  $\Omega_b = 0.04$ ). Other than the difference in  $h$ , we match these exactly. This normalization was calculated by ENF as an average X-ray emission weighted temperature of 10 clusters at  $z = 0$ .

Combining the normalization with the proportionality, we arrive at the final form of our M-T relation:

$$T = 6.59 \times 10^{-10} \left( \frac{M_{\text{vir}}}{M_{\odot}} \right)^{2/3} \left( \frac{\Delta(z)}{\bar{\Delta}(0)} \right)^{1/3} \left( \Omega_{\text{m},0}(1+z)^3 + \Omega_{\phi,0}(1+z)^{3(1+w)} \right)^{1/3} \left( \frac{h}{0.7} \right)^{2/3}, \quad (8)$$

where  $\bar{\Delta}(0)$  denotes the value of  $\Delta(z)$  for the fiducial model, and is not recalculated when we vary the cosmology to calculate derivatives. For now, we will assume that the evolution of the  $M-T$  relation is described (perfectly) by Eq. (8) over the range of redshift of relevance. We shall return to this point later.

### 3.3. Assembling the CMB and SNe Fisher matrices

To make our analysis more realistic, we have computed the Fisher matrices associated with CMB and SNe experiments, and added them as priors to the Fisher matrix obtained with a cluster survey. To compute the Fisher matrix associated with an experiment such as the upcoming MAP mission, we have used the methods described in Eisenstein *et al.* 1999 and have faithfully reproduced their constraints. Assuming Gaussian perturbations and noise the CMB Fisher matrix is given by

$$\mathbf{F}_{ij} = \sum_{\ell} \sum_{X,Y} \frac{\partial C_{X\ell}}{\partial \theta_i} (\text{Cov}_{\ell})_{XY}^{-1} \frac{\partial C_{Y\ell}}{\partial \theta_j} \quad (9)$$

$C_{X\ell}$  is the power in the  $\ell^{\text{th}}$  multipole and the indices X and Y run over T,E,B,C; the temperature, E-channel polarization, B-channel polarization and the temperature-E mode cross correlation. The matrix  $\text{Cov}_{\ell}$  depends on the  $C_{X\ell}$ , the beam window function, and detector noise levels. The explicit form of the matrix can be found in Eisenstein *et al.* 1999 where we have used the specifications for MAP at 90 GHz. We have optimistically assumed a sky coverage of 80%.

Calculating the Fisher matrix for a SNe experiment is a problem addressed recently in Tegmark *et al.* 1998. It depends on several observables; the number of SNe observed,  $N$ , the mean redshift of the observed SNe,  $\bar{z}$ , the scatter about this mean redshift,  $\Delta z$ , and the standard deviation in the observed magnitude from the predicted value  $(\Delta m)^2$ . Because we would like to use the constraints that will be obtained from future experiments such as SNAP, we also postulate a Gaussian distribution function  $f(z)$  of  $N$  supernovae distributed about  $\bar{z}$ . For a flat cosmology, the Fisher information matrix is given by

$$\mathbf{F}_{ij} = \frac{1}{(\Delta m)^2} \int_0^{\infty} f(z) w_i(z) w_j(z) dz, \quad (10)$$

where

$$w_i(z) = \left( \frac{5}{\ln 10} \right) \eta^{-1} \frac{\partial \eta}{\partial \theta_i}. \quad (11)$$

The  $\theta_i$  are the cosmological parameters to be constrained, and  $\eta$  is given by

$$\eta(a; \Omega_{\text{m}}, \Omega_{\phi}) = \int_a^1 \frac{da}{a^2 H(a)} \quad (12)$$

where  $H(a) \equiv H_0[\Omega_{\text{m}}a^{-3} + \Omega_{\phi}a^{-3(1+w_{\phi})}]^{1/2}$ .

We computed the SNe Fisher matrix for two different cases. First, we calculated the constraints given by a cautious estimate of 200 supernovae. They followed a Gaussian distribution at a mean redshift of 0.65 with a dispersion of 0.3 in redshift. The standard deviation in the observed magnitude was  $\Delta m = 0.3$ . We also considered a more optimistic survey, providing 400 supernovae with a mean redshift of 0.7 and a dispersion of 0.4 in redshift and  $\Delta m = 0.2$ . Both of these scenarios are relatively conservative when compared to the expected yield of around 2000 Supernovae to be observed by the proposed experiment SNAP. Both samples are used in the analysis below.

## 4. RESULTS

It is instructive to compare Fisher matrices obtained using different experimental setups. In this paper, we change the specifications of the cluster survey, and find the effect on the constraints obtained. An important question to consider is whether the limitations on improving a constraint are dominated by the experiment or the underlying theory, or some combination thereof. In the analysis, we have separated the two issues by parameterizing the theoretical uncertainty in the M-T relation, and including its normalization and scatter in the cluster Fisher matrix. To study experimental effects alone, we simply invert the Fisher matrix without any additional priors on the M-T relationship. To examine the effect of theory uncertainties, we add additional priors for the M-T normalization and scatter for a given experimental setup. Thus, we gain an intuition for which sources of error are the most significant.

An observational question that merits attention when designing the optimal cluster survey is the trade off between angular coverage on the sky, and depth of field of the survey,  $z_{\text{end}}$ . It would be nice to know whether the bulk of the constraint on a parameter is determined by the redshift evolution of the number density of clusters, or rather simply on the total number of clusters today. The former would suggest that a narrow, deep survey would be best, while the latter could easily be accomplished with a shallow survey with a wide angular coverage. In general, the constraint depends on both quantities, and the dominant effect depends upon the parameter being considered. We approach the question from the back by simulating both types of observations and plotting the dependence of the constraint on depth or angular coverage.

In our analysis of the various cluster surveys, we wish to consider not only the survey's constraining capabilities on its own, but also its ability to improve the constraints already obtained from observations of the CMB and type Ia Supernovae. To obtain combined constraints, one has simply to add the Fisher matrices together and invert the resulting matrix. In practice, using Cholesky decomposition (Press *et al.* 1986) to calculate the inverse is somewhat unstable because the fiducial parameters vary by many orders of magnitude. This instability is avoided by performing the analysis on the logarithms of the cosmological parameters. Since the Fisher matrix transforms as a covariant tensor under a variable change in parameter space,

this modification is easily accomplished using the Jacobi matrix.

The  $i$ th diagonal element of the inverse of the sum of the three Fisher matrices gives a lower bound on the  $1 - \sigma$  error bars obtained from all three experiments. When the other parameters are allowed to vary:

$$\Delta\theta_i^2 \geq (\mathbf{F}^{-1})_{ii}. \quad (13)$$

This relation accommodates the propagation of errors in different parameters, since inverting the Fisher matrix is equivalent to marginalizing over all of the other parameters. We define the *optimal percent constraint* as the minimum  $\Delta\theta_i/\theta_i$  allowed by equation 13, which is interpreted as the size of the  $1 - \sigma$  error bar.

However, the Fisher matrix also quantifies the covariance of the parameters. For each type of observation, a realistic picture of its capabilities is obtained by plotting elliptical curves of constant likelihood using a 2 parameter subspace of the inverted Fisher matrix. This view explicitly depicts the degeneracies discussed in §2 between the two displayed parameters, while marginalizing over all the rest. These degeneracies can be broken if the curves of constant likelihood from other experiments are oriented in an orthogonal direction, since adding the Fisher matrices effectively multiplies the likelihoods. Figure 1 displays the  $1 - \sigma$  regions of likelihood for all three individual experiments, and also the combined constraint, illustrating the efficacy of this technique. Table 1 contains the  $1 - \sigma$  errors on each of the parameters after combining the CMB matrix (using specifications of MAP with polarization), 200 supernovae matrix (about a mean redshift of 0.65), and a cluster survey of 1000  $\text{deg}^2$  with temperature threshold 5 keV to a limiting redshift of  $z_{\text{end}} = 0.7$ .

Table 1 reveals an interesting phenomenon; the X-ray cluster survey constrains the normalization of the M-T relationship, if its redshift evolution is assumed known. Without any prior information about the normalization of the the M-T curve from simulations, a constraint of reasonable order can be achieved observationally. The constraint on the scatter  $\sigma_{M-T}$  is not as good. This indicates that unless theory can predict the M-T normalization to better than  $\sim 20\%$ , prior knowledge of the normalization will not significantly alter the results (see e.g. Pierpaoli, Scott, & White 2001). Prior knowledge of the scatter appears to be even less significant. We quantitatively investigate this below (see Figure 7).

The orientation and size of the cluster ellipse in Figure 1 depends on the depth and angular extent of the survey. The change in orientation in the  $\Omega_m - w_\phi$  plane has been noticed previously (Hu & Kravtsov 2002). That the size will decrease with increasing depth is apparent; more information will result in a better constraint. Figure 2 demonstrates how the orientation of the ellipse changes in a progression from a shallow survey to a deep one at fixed angular size. These plots do not contain information from either the CMB or the SNe. However, the number density of clusters at a given redshift is a quantity which is largely insensitive to the parameter  $\Omega_b h^2$ . This causes the Fisher Matrix to be almost singular, reflecting the large degeneracy in that direction. Thus we do rely on results from Big

Parameter	Fiducial value	$1 - \sigma$ error
$\Omega_m$	0.3	10.3%
$h$	0.67	2.67%
$\Omega_b h^2$	0.0254	3.86%
$n_S$	1	2.58%
$w_\phi$	-1	8.90%
$\delta_H$	$5.02 \times 10^{-5}$	5.05%
$T/S$	0	$\pm 0.796$
$\tau$	0.2	17.5%
M-T norm	$6.59 \times 10^{-10}$	15.4%
$\sigma_{M-T}$	0.1333	138%

TABLE 1

The errors in each parameter from a combination of a CMB, SNe, and cluster survey of 1000  $\text{deg}^2$  to a depth of  $z=0.7$ . Percent errors are given in terms of the fiducial values.

Bang Nucleosynthesis to provide us with a 10% prior on this quantity, which we include throughout our analysis for greater numerical stability. Note that the shape converges for the deepest surveys, as fewer and fewer clusters above the detection threshold are detected.

The change in the orientation of the direction of degeneracy is a direct consequence of the fact that cluster surveys probe a combination of the proper distance and the growth function. In the range  $0 < z < 0.5$ , the proper distance to adjacent redshift bins is a quickly varying function, and thus the sensitivity to small changes in the cosmological parameters is dominated by changes in this proper distance. Hence, the direction of degeneracy of these shallow cluster surveys tend to align with contours of constant proper distance, as can be seen in the first panel of Figure 2. In the high redshift range  $z > 1$  however, each

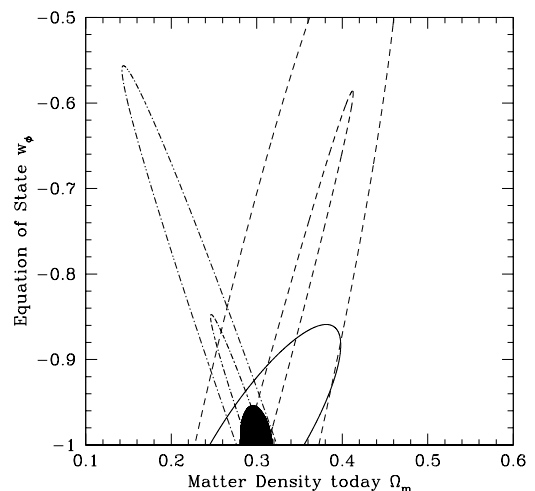


FIG. 1.—  $1 - \sigma$  regions of maximum likelihood in the  $\Omega_m - w_\phi$  plane. Constraints come from a cluster survey of 1000  $\text{deg}^2$  to a final redshift of 1.2 and temperature threshold 5 keV (solid), observations of the CMB (dashed) using the specifications of MAP (outer) and PLANCK (inner) including the polarization information, and finally a hypothetical supernova observation (dot-dashed) with 200 (outer) and 400 (inner) supernovae. The solid contour is the joint constraint from the cluster survey, 200 supernovae, and MAP.

redshift bin adds an increasingly large number of clusters. The number of collapsed objects at high redshift is very sensitive to the growth function, and thus in this redshift regime, the direction of degeneracy aligns instead with the contours of constant growth factor, normalized to today. This leads to an interesting detail: populations of different masses will come to be dominated by the growth factor at different redshifts. This is because of the hierarchical nature of structure formation. More massive clusters form later, and thus massive clusters get rarer faster as deeper redshifts are probed. The more massive populations get dominated by the growth function at smaller redshifts. We have determined that the higher the temperature threshold, the lower the final redshift  $z_{\text{end}}$  at which one runs completely out of clusters;  $z_{\text{end}} \sim 1$  for 8 keV and  $z_{\text{end}} \sim 1.6$  for 5 keV (see Figure 2), while  $z_{\text{end}}$  is far beyond 2 if one stretches the threshold to 3 KeV. The orientations of the constraints at these limits are also slightly different, being most orthogonal to CMB and supernova constraints for the smaller objects. One complication is that the lower the temperature threshold is extended, the more one has to worry about extra physics that may affect the low mass systems, but are difficult to theoretically model. These considerations must be traded off with depth and angular coverage when a survey is being planned. The optimal strategies clearly depend on the capabilities of the surveying technique, which we discuss below.

By far the easiest experimental specification to examine is the angular coverage of the survey. Changing the angular coverage effectively changes the volume element at each redshift  $z$ . As the Fisher matrix contribution from the cluster survey is linearly dependent on its volume, and the volume is, in turn, linearly dependent on the survey's angular size, the parameter constraints solely from the cluster survey go as:

$$\Delta\theta \propto \frac{1}{\sqrt{S}} \quad (14)$$

where  $S$  is the solid angle subtended by the survey, where for a full sky survey  $S$  is  $4\pi/41000$ . The volume element also depends on the comoving distance, which is a function of the cosmological parameters. Figure 3 shows the improvement in the constraint on the matter density  $\Omega_m$  for the three experiments as the angular size of the survey

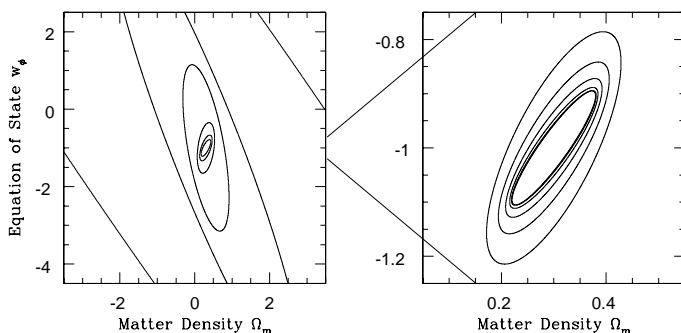


FIG. 2.—  $1 - \sigma$  regions of maximum likelihood in the  $\Omega_m - w_\phi$  plane for a series of cluster surveys differing only in survey depth. In the left hand panel, constraints are plotted for  $z_{\text{end}} = 0.1, 0.2, 0.3, 0.5, 0.7, 0.9$  decreasing in size. The right hand panel has  $z_{\text{end}} = 0.9, 1.1, 1.3, 1.5, 1.7, 1.9$ .

increases. The relation is not quite as simple as in equation 14 because of the prior information provided by the CMB and Supernovae.

What we notice is that if the survey is deep enough there seems to be a “sweet spot”, a clear cutoff place where the effort involved in performing the survey returns maximum scientific information, and beyond which the payoff is not high. For example, for survey depth  $z_{\text{end}} = 1.2$  the payoff for extending the observations from 500 to 2000  $\text{deg}^2$  is quite considerable, but extending the survey to  $10^4 \text{ deg}^2$  does not improve the optimal constraint significantly from a survey of  $\sim 2000 \text{ deg}^2$ . It is important to keep this turning point in the back of one's mind because increasing the angular coverage greatly increases the total number of clusters that need to be observed.

Another strategy to consider is to make the survey deeper rather than wider. In this case there may be a smaller total sample of clusters, but the evolution of the number density will be more apparent. In Figure 4, the dependence of the constraint on the matter density is displayed as a function of  $z_{\text{end}}$ , the depth of the survey. Of course many surveys are flux limited, and thus the depth of the survey is different for different mass scales; brighter more massive objects can be seen at greater distance. However, since a significant portion of the constraint comes from the evolution of the density of clusters, and not just from the total number, it is crucial that the sample be complete. Therefore, the depth of the survey is effectively the one at which completeness is achieved for the faintest objects being counted, and we will assume this in our analysis. In practice this depth will depend on the type of survey, and of course on the temperature threshold  $T_{\text{min}}$ . Constraints in Figure 4 are shown from the cluster survey alone, the cluster survey combined with the expected constraint from the CMB MAP mission (with polarization information), and finally from the cluster sur-

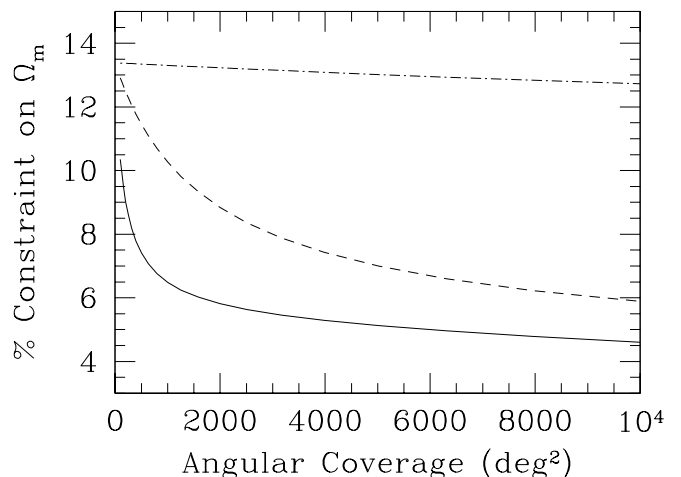


FIG. 3.— The percent constraint on  $\Omega_m$  as a function of the angular coverage of the cluster survey. We have added the Fisher matrices from the MAP CMB experiment, and from 200 supernovae, as well as a 10% prior on  $\Omega_b h^2$  from BBN. The solid line is a survey to depth  $z_{\text{end}} = 1.2$ , the dashed line is a survey to  $z_{\text{end}} = 0.7$ , and the dot-dashed line has a depth of  $z_{\text{end}} = 0.3$ .

vey combined with both the CMB and SNe experiments.

Again what we see is that there is a definite “sweet spot.” The role of the prior information matrices of the SNe and CMB experiments is also apparent in this graph. The flat nature of both of the dot-dashed curves between  $z_{\text{end}} = 0$  and  $z_{\text{end}} \sim 0.5$ , which incorporate the constraints from all three types of experiments, are a result of the fact that although the survey is getting deeper and the number of clusters detected is growing, the constraint from the cluster survey is weak compared to combined constraints from the CMB and SNe. The solid curve displaying the cluster constraint alone shows that this is true. In terms of the elliptical plots above, the likelihood contours from CMB experiments would be entirely within the region of maximum likelihood determined by the cluster survey. After  $z_{\text{end}} = 0.5$  we see a marked improvement, which means the likelihood contour will have become small enough to intersect the CMB and SNe contour in a way that decreases the most probable region compatible with all the experiments. Not only has the size of the cluster constraint decreased significantly by  $z_{\text{end}} \sim 0.5$ , but as one can see from Figure 2 the orientation has passed the vertical and becomes increasingly orthogonal to the other constraints between  $0.5 < z_{\text{end}} < 1.7$ . The role of the SNe constraint is also clear. 400 supernovae provide a narrower lever arm in parameter space than 200. Since both SNe contours are at a significant angle to the cluster constraints, and since they intersect at the position of the fiducial model (by fiat), then the effect is simply to decrease the area of the intersecting region by an approximately constant amount, which can be observed in Figure 4.

Another interesting property of experiments that should be carefully studied is the effect of changing the detection threshold temperature on the quality of the constraints

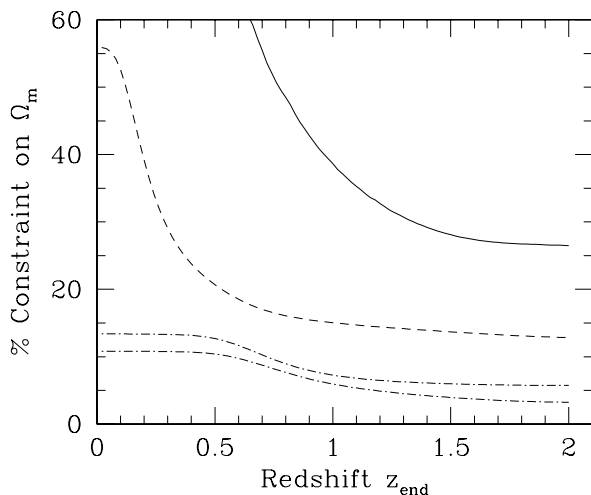


FIG. 4.— The percent constraint on  $\Omega_m$  as a function of the depth of the cluster survey. This survey has an angular coverage of  $1000 \text{ deg}^2$ . The solid line is the constraint from the cluster survey combined with the 10% BBN prior. The dashed line is obtained when the results of the CMB (MAP), cluster observations, and BBN prior are added, and finally the dot-dashed lines are the constraints obtained when all three types of observations are used; the cluster survey, the CMB, and either 200 (upper) or 400 (lower) SNe, also with the BBN prior.

that can be obtained. In some types of surveys this could be intimately related to the depth of the survey, for example if the survey was flux limited, since flux correlates with temperature. However this is not always true. In the case of the SZE effect, the limiting temperature is largely independent of redshift. Also for X-ray surveys one could argue that those clusters for which accurate temperatures can be known are well above the flux limit, allowing essentially volume limited samples to be constructed. Since temperature can be used as a proxy for mass, studying this dependence is akin to asking whether most of the constraint comes from the rare high mass clusters, or whether the large number of lower mass clusters are needed in order to adequately constrain the parameters. We would prefer the former scenario, because the higher  $T_{\text{min}}$ , the less sensitive are the results to non-gravitational physics in the modeling, and the easier it is to make the observations. The value of  $T_{\text{min}}$  has a strong nonlinear effect on the number of objects that will be found within the domain of the survey, as Figure 5 shows. Figure 6 illustrates the improvement in our knowledge of the matter density as we lower the threshold temperature.

This clearly demonstrates that it is indeed the rarest high mass clusters that contribute the bulk of the constraint. For a survey out to  $z_{\text{end}} = 1.2$ , if one drops the threshold halfway down the range of the plot, from 8 keV to 5 keV, then one adds about 800 clusters and improves the constraint by a factor of 3/4 the original value. If one considers the bottom half from 5 keV to 2 keV, one adds  $\sim 24,000$  clusters, yet only improves the constraint by another factor of 3/4. If all clusters were equally important in constraining  $\Omega_m$  then the constraint would drop significantly more in the bottom half of the plot, because we have increased the number of clusters surveyed by more than an order of magnitude.

It is useful to probe how strongly the constraint on  $\Omega_m$  (or any other parameter) depends on the theory implicit in the survey. Many cluster surveys involve observation of the

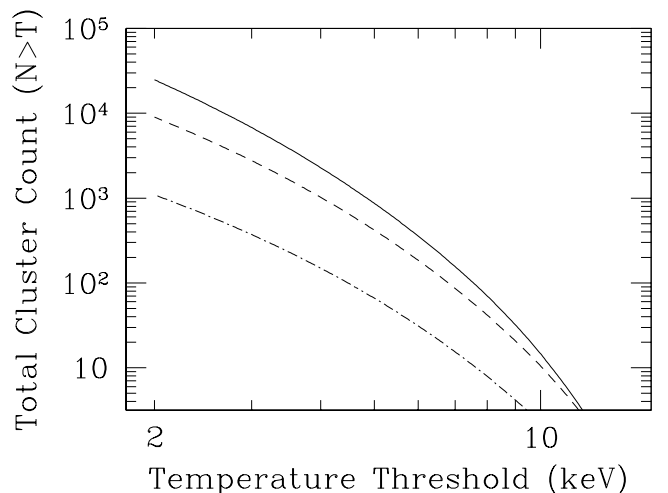


FIG. 5.— The total number of clusters detected at all redshifts out to  $z_{\text{end}} = 1.2$  (solid),  $z_{\text{end}} = 0.7$  (dashed) and  $z_{\text{end}} = 0.3$  (dot-dashed) as a function of the detection threshold in keV for a fixed angular aperture of  $1000 \text{ deg}^2$ .

X-ray luminosity or temperature, either because they are X-ray surveys, or else they are optical or SZE surveys that require an X-ray followup to obtain redshift and temperature information. For a cluster survey in X-ray temperature, this uncertainty is framed in terms of the uncertainty in the normalization and the scatter about the mass temperature relationship. It is conceivable that adding more clusters to the survey will not affect the constraint on  $\Omega_m$  simply because the Fisher matrix is dominated by the error from the M-T normalization and scatter. If this is the case, considerable effort should be invested in improving these theoretical considerations, so as to use the plethora of upcoming data to maximum advantage.

By including the M-T normalization and scatter as parameters in the Fisher matrix, we have investigated this important issue. We find that precise knowledge of the scatter about the M-T relationship does not significantly improve the quality of the constraint on  $\Omega_m$ . Reducing the prior on the scatter in a survey to  $z_{\text{end}} = 0.7$  from a very loose prior of 100% to an extremely tight 5% improved the constraint on the matter density less than 1%, with a 10% BBN prior and the CMB and 200 SNe experiments included. The improvement of the constraint on  $\Omega_m$  with better knowledge of the M-T normalization is of the same order when the prior is changes from 10% to 1%. Weaker priors on the normalization have little effect because the cluster survey constrains it to 15% by itself (Table 1). Figure 7 shows this dependence for several redshifts.

## 5. CONCLUSIONS

Many exciting surveys of galaxy clusters have been proposed, involving several different observational techniques to locate the clusters. In this paper we have analyzed their potential to constrain two of the most fundamental cosmological parameters,  $\Omega_m$  and  $w_\phi$ , within a larger framework of information gathered from other types of observations. We have considered the effects of theoretical uncertain-

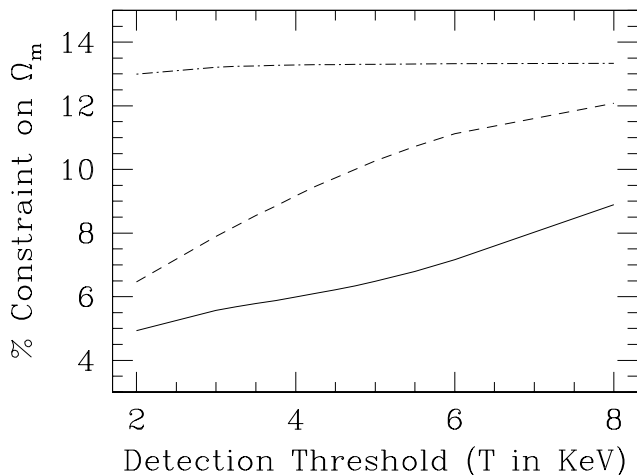


FIG. 6.— The percent constraint on  $\Omega_m$  as a function of the temperature detection threshold. We have added the same priors as in the previous two figures. The solid line is a survey to depth  $z_{\text{end}} = 1.2$ , the dashed line is a survey to  $z_{\text{end}} = 0.7$ , and the dot-dashed line has a depth of  $z_{\text{end}} = 0.3$ .

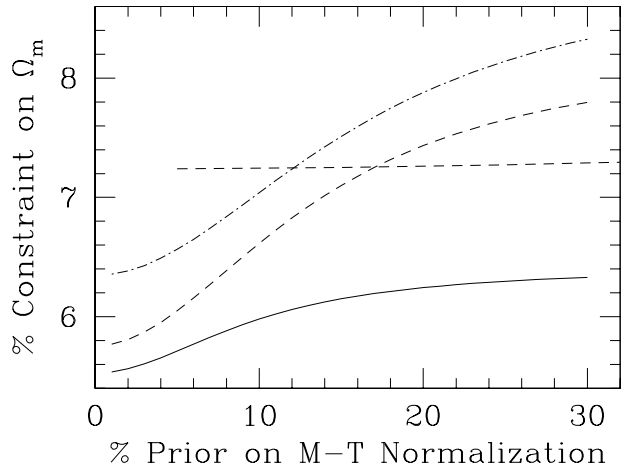


FIG. 7.— The percent constraint obtained for  $\Omega_m$  as a function of the prior knowledge of the error bar on the normalization of the M-T relation, also reported in percent. The solid line is a survey to depth  $z_{\text{end}} = 1.2$ , the dashed line is a survey to  $z_{\text{end}} = 0.7$ , and the dot-dashed line has a depth of  $z_{\text{end}} = 0.3$ . We have also shown the change of constraint as a function of the prior knowledge of the scatter from the M-T relation for  $z_{\text{end}} = 1.2$ . The constraint does not depend strongly on this quantity.

ties on these constraints. Even when the equation of state  $w_\phi$  is postulated to be a constant, large degeneracies exist in the  $\Omega_m - w_\phi$  subspace from all types of observations studied here. We have varied some of the characteristic attributes of cluster surveys such as the limiting temperature threshold, the depth of the survey, and the angular coverage, and have noted that the direction of elongation of the elliptical region of maximum likelihood depends considerably on these attributes. Since we know the direction of degeneracy for other important experiments, we can use this information to optimize the cluster survey strategy, taking into account the various limitations for X-ray followup observations.

We have deduced that in order to achieve maximal sensitivity to  $\Omega_m$ , with minimal sensitivity to  $w_\phi$  (without taking into account CMB and SNe experiments), a fairly shallow survey to  $0.4 < z_{\text{end}} < 0.7$  (depending on the limiting temperature used) with large angular coverage is an effective approach, because in this case the constraint ellipse is vertically oriented in the  $\Omega_m - w_\phi$  plane. It would be interesting for future work to see if such a constraint would be relatively independent of  $w'_\phi$ . If so, such a measurement would yield a significant lever arm to experiments such as SNAP, who would then be in a good position to tighten constraints on  $w'_\phi$ . We also found that for a survey of fixed angular extent, the clusters with the highest constraining power are those with high temperature. We confirm the claim made by Holder *et al.* 2001 that it is the clusters past  $z > 0.5$  that provide most of the constraint on  $\Omega_m$  (given our assumption that  $\Omega_m + \Omega_\phi = 1$ ). This is especially evident when SNe and CMB experiments are combined with the cluster survey, because the part of the cluster constraint that is orthogonal to the SNe and CMB ellipses comes from the clusters located at  $z > 0.5$ . We also see a natural cutoff in limiting redshift beyond which



the constraint on  $\Omega_m$  stops improving, as the number of clusters hotter than the detection threshold falls off steeply with  $z$ . More surprisingly, we also find that when the cluster survey is combined with the CMB and SNe constraints, increasing the field of view of the survey does not improve the results indefinitely.

In summary, when designing an experiment, several competing effects must be accounted for. If one is interested in constraining  $\Omega_m$  and  $w_\phi$  simultaneously, then maximizing orthogonality with the CMB and Supernova constraints is desirable because it will maximize the return for each unit of observing time that is spent counting objects. In general this suggests that deep surveys are advantageous because it is at high redshifts that the growth function significantly affects the number density of clusters. If an observable such as the SZ effect can truly probe out to very high redshifts with relative completeness, then it is also advantageous to stretch the temperature threshold as low as possible, since this allows a deeper effective depth before the clusters run out. The resulting difference in angle is a relatively small effect however, and naturally there are limits to the practicality of lowering the threshold. The number of dim distant objects that would need to be followed up grows exponentially as the threshold decreases. To some extent, this can be compensated by making the survey narrower.

If, on the other hand, the survey is flux limited and can probe completely only to a relatively shallow  $z_{\text{end}}$ , such as an optical or X-ray survey of clusters, the optimal strategy changes. In this case we take advantage of the fact that very massive clusters are dominated by the growth function at smaller redshifts. For maximum orthogonality in shallow surveys, one raises the temperature threshold and studies only the most massive clusters. We have shown that this will not significantly weaken the survey's performance since typically the more massive clusters contribute the bulk of the constraining power. Of course to compensate for the fact that huge cluster are rather rare, the survey can be widened, keeping in mind that for each  $z_{\text{end}}$ , there is a point of diminishing returns when doing this.

In investigating different survey techniques' abilities to effectively whittle down the likely region obtained from SNe and CMB experiments, we have been conservative about the theoretical uncertainties involved in connecting the observable (X-ray temperature) to the quantity predicted by the theory (cluster mass). We have included the normalization and scatter as parameters in our Fisher Matrix analysis. Any error in these parameters propagates to the constraints on the cosmological parameters. We have investigated the sensitivity of our constraints on  $\Omega_m$  and  $w_\phi$  to errors in the normalization and scatter of the M-T relation by including prior constraints on these quantities and observing the improvement on the parameter constraints. We found that in general, the constraints on  $\Omega_m$  and  $w_\phi$  are fairly robust against large errors in the scatter of the M-T relation, but that they do depend somewhat more strongly on errors in the normalization. It is interesting that if no priors are added, the cluster survey itself will constrain the normalization to around 10%, suggesting that cluster surveys could lead to some insight into intrin-

sic cluster properties. We have not addressed what might happen if non-Gaussian effects were to account for a large portion of the error on M-T, nor have we accommodated a normalization that changes with redshift. These would change the shape of the temperature-redshift distribution and could impact the determination of the cosmological parameters profoundly. To assess the impact of the first it would be necessary to employ a monte-carlo method, rather than the simple Fisher matrix techniques used in this paper. To understand quantitatively the question of evolution is beyond the scope of this work.

It is clear that surveys of galaxy clusters will play a key role in the future of further constraining the cosmological parameters. Tight constraints on  $\Omega_m$  and the evolution of the dark energy are essential to developing our models of the universe. A precise determination of  $\Omega_m$  will help quantify the dark matter problem, and aid in solving questions of structure formation. The more  $\Omega_m$  can be independently constrained, the better leverage we will have later when observations of very deep sources begin to give us more information about the evolution of the dark energy.

#### ACKNOWLEDGMENTS

The authors would like to thank Daniel Eisenstein for his assistance regarding the CMB Fisher matrix, and Saul Perlmutter for his useful insights. Also thanks to J.D.Cohn, C. Metzler, and J. Mackey for the many clarifying discussions on this work. This research was supported in part by the Harvard College Research Program (ESL), a Sloan Fellowship and the National Science Foundation.

#### REFERENCES

- de Bernardis, P., et al., 2001, preprint [astro-ph/0105296]
- Bond, J.R., & Myers, S., 1996, ApJS **103**, 41
- Bryan, G., & Norman, M., 1986, ApJ **495**, 80
- Cohn, J.D., 1998, Ap&SS **259**, 213 [astro-ph/9807128]
- Efstathiou, G., Frenk, C.S., White, S.D.M., & Davis, M., 1988, MNRAS **235**, 715
- Efstathiou, G., & Rees, M., 1988, MNRAS **230**, 5P
- Eisenstein, D.J., & Hu, W., 1997, ApJ **511** 5 [astro-ph/9710252]
- Eisenstein, D.J., Hu, W., & Tegmark, M., 1998, ApJ **518**, 2 [astro-ph/9807130]
- Eke, Vincent R., Cole, Shaun, & Frenk, Carlos S., 1996, MNRAS **282**, 263 [astro-ph/9601088]
- Eke, Vincent R., Navarro, Julio F., & Frenk, Carlos S., 1998, ApJ **503** 569 [astro-ph/9708070]
- Evrard, August E., Metzler, Christopher A., & Navarro, Julio F., 1996, ApJ **469**, 494 [astro-ph/9510058]
- Gelb, J., & Bertschinger, E., 1994, ApJ **436**, 467.
- Haiman, Z., Mohr, J.J., & Holder, G.P., 2000, ApJ **553** 545 [astro-ph/0002336]
- Hanany, S., et al., 2000, ApJ **545**, L1 [astro-ph/0005124]
- Henry, J.P., 2000, ApJ **534**, 565
- Holder, G.P., Haiman, Z., & Mohr, J.J., 2001, preprint [astro-ph/0105396]
- Hu, W., Eisenstein D.J., Tegmark, M., & White M., 1999, PRD **59**, 3512
- Hu, W., & Kravtsov, A. 2002, preprint [astro-ph/0203169]
- Huterer, D., & Turner, M.S., 2001, PRD **64**, 123527
- Jenkins, A., Frenk, C.S., White, S.D.M., Colberg, J.M., Cole, S., Evrard, A.E., Couchman, H.M.P., & Yoshida, N., 2001, MNRAS **321**, 372 [astro-ph/0005260]
- Kaiser, N., 1986, MNRAS **222**, 323
- Kneissl, R., et al., 2002, MNRAS **328**, 783
- Lacey, C., & Cole, S., 1994, MNRAS **271**, 676
- Miller, A.D., et al., 1999, ApJ **524**, L1
- Newman, J.A., Marinoni, C., Coil, A.L., & Davis, M., 2002, PASP **114**, 29

- Oukbir, J., & Blanchard, A., 1992, *A&A* **262**, L21
- Padin, S., et al., 2001, *ApJ* **549**, L1-L5 [astro-ph/0012211]
- Peacock, J.A., 2000, *Cosmological Physics*, CUP
- Perlmutter, S., Turner, M., & White, M., 1999, *Phys. Rev. Lett.* **83**, 670
- Pierpaoli, E., Scott, D., & White, M., 2001, preprint [astro-ph/0010039]
- Pierre, M., Valtchanov, I., & Refregier, A., 2002, preprint [astro-ph/0202117]
- Podariu, S., & Ratra, B., 2001, *ApJ* **563**, 28.
- Press, W.H., Flannery, B.P., Teukolsky, S.A., & Vetterling, W.V., 1986, *Numerical Recipes*, CUP
- Press, W.H., & Schechter, P., 1974, *ApJ* **187** 425
- Pryke, C., et al., 2001, preprint [astro-ph/0104490]
- Romer, A.K., Viana, P.T.P., Collins, C.A., Liddle, A.R., Mann, R.G., & Nichol, R.C., 2001, preprint [astro-ph/0111131]
- Sheth, R., & Tormen, G., 1999, *MNRAS* **308**, 119
- Smoot, G.F., et al., 1992, *ApJ* **396**, L1
- Spergel, David N., & Starkman, Glenn D., preprint [astro-ph/0204089]
- Sunyaev, R., & Zel'dovich, Ya.-B., 1980, *ARA&A* **18**, 537
- Tegmark, M., Eisenstein, D.J., Hu, W., & Kron, R.G., 1998, preprint [astro-ph/9805117]
- Tegmark, M., Taylor, A.N., & Heavens, A.F., 1996, preprint [astro-ph/9603021]
- Viana, Pedro T., & Liddle, Andrew R., 1999, *MNRAS* **303**, 535 [astro-ph/9902245]
- White, M., 1998, *ApJ* **506**, 495 [astro-ph/9802295]
- White, S.D.M., Efstathiou, G., & Frenk, C., 1993, *MNRAS* **262**, 1023